Oscillations and Mechanistic Analysis of the Chlorite−Sulfide Reaction in a Continuous-Flow Stirred Tank Reactor

Shancheng Mao,[†,‡] Qingyu Gao,*[,†,§] Hai Wang,[†] Juhua Zheng,[†] and Irving R. Epstein*[,§]

College of Chemical Engineering, China University of Mining and Technology, Xuzhou 221008, People's Republic of China, College of Life Sciences and Chemical Engineering, Huaiyin Institute of Technology, Huaian 223003, People's Republic of China, and Department of Chemistry and Volen Center for Complex Systems, MS 015, Brandeis University, Waltham, Massachusetts 02454-911

Received: September 2, 2008; Revised Manuscript Received: December 5, 2008

Sustained oscillations in pH and redox potential are found in the chlorite−sulfide reaction in a continuous-flow stirred tank reactor (CSTR). Autocatalytic oxidation of HSO_3^- by ClO_2^- is the major source of positive feedback of hydrogen ions. The reaction between H_2S and ClO_2^- to form S_8, which consumes H^+, is an important source of negative feedback. A model consisting of five protonation−deprotonation equilibria and nine redox reactions is proposed for the oscillatory reaction between S^{2-} and ClO_2^-. The 10 species included are HS^-, H_2S, $S_2O_3^{2-}$, SO_3^{2-}, HSO_3^-, OCl^-, HOCl, ClO_2^-, H^+, and OH^-. In contrast to the H_2O_2−S^{2-} oscillatory reaction, $S_2O_3^{2-}$ is shown here by capillary electrophoresis to be an important intermediate. Simulations give qualitative agreement with the pH oscillatory behavior observed in the CSTR.

Introduction

As an important reducing reagent, sodium sulfide is widely used in hydrometallurgy, ore dressing, and Kraft cooking as well as in batteries and photoelectrochemical cells.[1−4] Most of these processes involve the oxidation of sulfide to give a variety of products such as polysulfide, elemental sulfur, and sulfur oxyanions, depending on the conditions. Hydrogen sulfide, which is produced during the hydrolysis of sulfide ion generated by industries such as tanning, pulp, paper, mining, and oil and gas drilling, is a dangerous pollutant that is toxic to humans and can significantly damage metallic materials. Consequently, various methods and strategies, including chemical, biological, and electrochemical oxidation, have been applied to detect, control, and remove sulfide from wastewater.[5] Thus, better understanding of the nature of sulfide oxidation is critical both for improving its applications and for pollution control. In the past three decades, a great deal of attention has been focused on the oxidation of sulfide by oxygen,[6] hydrogen peroxide,[7,8] bromate,[9] persulfate,[10] and chlorite[11] and via electrochemical methods,[12] and various nonlinear phenomena have been discovered in these reactions.

Sodium chlorite, which is widely used in disinfecting drinking water, is a strong oxidant. It can be reduced by various molecules, including sulfur-containing species such as thiourea,[13−16] thiosulfate,[17−20] thiocyanate,[21] sulfite,[22] and tetrathionate.[23] Due to its relevance to both industrial processes and academic research, the redox reaction between chlorite and S(-II) species has been investigated extensively during the past three decades. The first hint that oscillatory phenomena may arise in reactions between chlorite and sulfur-containing species goes back over a quarter century,[17] and intense research on temporal and spatial pattern formation in this class of reactions has been carried out since then.

Although significant progress has been made toward understanding the nonlinear dynamics of chlorite−sulfur(-II) reactions, sustained oscillatory phenomena have not previously been reported in the chlorite−sulfide system. The first nonlinear phenomena observed in the chlorite−sulfide−sulfuric acid reaction in a batch reactor were reported by Rushing et al.[11] The oligo-oscillations they found lasted for only 15 s. Orbán[24] found sustained oscillations in a chlorite−sulfide system augmented with catalytic amounts of Cu(II) in a CSTR. To our knowledge, there is no subsequent report of sustained oscillations in the two-species system in the absence of additional redox reagents or catalysts. Motivated by the importance of this reaction and the intriguing results of Rushing et al.,[11] we have investigated the reaction between chlorite and sulfide with three objectives: (1) exploring whether there are conditions under which sustained oscillations can occur; (2) deriving new insights into the mechanism of the chlorite−sulfide reaction; and (3) proposing and testing a detailed mechanistic model for this system.

Experimental Section

Na_2S and H_2SO_4 used in this work were analytical-reagent grade and were used without further purification. Sodium chlorite purchased from Aldrich (80%) was recrystallized twice from 75% acetone aqueous solution in the temperature range between −20 and 30 °C. After this treatment, the purity of chlorite reached 98.2% as determined by iodometric titration. The stock solution of sulfide was prepared frequently and was stored under nitrogen. Its concentration was determined by iodometric titration.

All solutions were prepared with deionized water (ultrafiltered from a Millipore system, 18.2 MΩ). Experiments were conducted in a continuous-flow stirred tank reactor (CSTR) thermostatted with a circulating water bath. The plexiglass reactor had a volume of 30.0 mL. Solutions of Na_2S (bubbled with nitrogen (>99.9%)), H_2SO_4, and $NaClO_2$ were separately transferred to the reactor by an ISMATIC (Switzerland) high precision pump. The solutions were mixed with a magnetic

[†] China University of Mining and Technology.
[‡] Huaiyin Institute of Technology.
[§] Brandeis University.

10.1021/jp807802v CCC: $40.75
Published on Web 01/21/2009

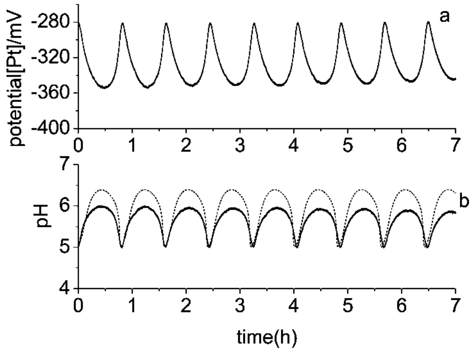

Figure 1. Sustained periodic oscillations in Pt potential (a) and pH (b) measured in the chlorite−sulfide system in a CSTR. $[Na_2S]_0 = 7.3 \times 10^{-4}$ M, $[NaClO_2]_0 = 8.8 \times 10^{-4}$ M, $[H^+]_0 = 3.7 \times 10^{-4}$ M, $k_0 = 0.73 \times 10^{-3}\ s^{-1}$, and $T = 32$ °C. Dashed line, simulations using the model in Table 1; solid line, experimental results.

stirrer (600 rpm). The initial concentrations of the reactants ($[S^{2-}]_0$, $[ClO_2^-]_0$, and $[H_2SO_4]_0$) are defined as the concentrations in the reactor after mixing in the absence of reaction. In the present case, the initial concentrations are one-third of the concentrations of the stock solutions of the three reactants. We also performed batch experiments, in which the reagents were mixed in the following order: sulfide, sulfuric acid, chlorite. The reaction was followed by UV−vis spectroscopy (Lambda 40, Perkin-Elmer) at 355 nm, a wavelength suitable for detecting chlorine dioxide.

The pH and redox potential were simultaneously measured with a glass electrode and a platinum electrode, respectively, coupled to a $Hg|Hg_2SO_4|K_2SO_4$ reference electrode. Signals from the reaction were recorded with an IBM PC through a Powerlab/4sp interface (AD Instruments, Australia). Before each series of experiments, a three-point calibration of the pH meter was performed with the use of standard buffer solution (pH 4.00, 6.00, and 9.18).

Capillary electrophoresis (CE) analysis was performed on a P/ACE MDQ (Beckman) instrument equipped with a diode array detector (DAD). A fused-silica capillary of 57.0 cm (50.0 cm to the detector) × 75 μm i.d. × 375 μm o.d. was used. The sample was injected into the capillary by an overpressure. A negative voltage of 25 kV was applied for separation, and a wavelength of 214 nm was selected for the spectrophotometric detection.

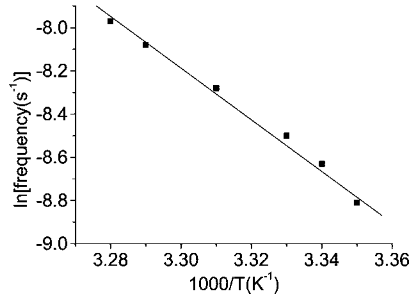

Figure 2. Arrhenius plot of the oscillatory frequency. $[Na_2S]_0 = 5.0 \times 10^{-4}$ M, $[NaClO_2]_0 = 1.2 \times 10^{-3}$ M, $[H^+]_0 = 2.2 \times 10^{-4}$ M, and $k_0 = 0.50 \times 10^{-3}\ s^{-1}$.

Results and Discussion

1. Experimental Results. Figure 1 shows regular sustained oscillations in the pH and redox potential at 32 °C. The peak-to-peak amplitudes are ~70 mV for the Pt electrode and 1.0 pH unit for the glass electrode. The oscillatory period is rather long, ~0.8 h. When the potential of the Pt electrode reaches its maximum value, approximately −280 mV, the pH takes its minimum value, ~5.0.

Temperature is found to have a significant effect on the oscillatory behavior. Although the waveform does not change, increasing the temperature accelerates the reaction and leads to a decrease in the oscillation period. Figure 2 plots the logarithm of the oscillation frequency (reciprocal of the period) versus the reciprocal of the reaction temperature between 25 and 32 °C. The frequency increases from 0.14 to 0.34 mHz over this range and shows Arrhenius-like behavior. If the temperature is increased to 34 °C, the oscillatory behavior disappears, and a low pH stable state is observed.

Figure 3 shows the dynamic phase diagram for this system. Oscillations are found in a narrow straplike region between 0.43 and 0.83 mM for $[S^{2-}]_0$ and between 0.20 and 0.50 mM for $[H^+]_0$. If $[H_2SO_4]_0/[S^{2-}]_0$ is kept at ~0.23, oscillations can be observed when the initial concentration ratio of ClO_2^- and S^{2-} lies between 1.2 and 2.0. In our experiments, the maximum oscillation amplitude was ~1.0 pH unit and 80 mV for the Pt electrode, a much larger range than observed in the unbuffered chlorite−thiourea system,[16] in which the amplitude varies between 0.1 and 0.3 pH units.

TABLE 1: Composite Reactions, Empirical Rate Laws, and Rate Constant Values for the Oscillatory Chlorite−Sulfide−Sulfuric Acid Reaction

no.	reaction	rate laws	rate constant (fitted or ref)
1	$HS^- + ClO_2^- \rightarrow 1/8S_8 + OH^- + OCl^-$	$r_1 = k_1[HS^-][ClO_2^-]$	$k_1 = 0.02\ M^{-1}\ s^{-1}$ (fitted)
2	$H_2S + ClO_2^- \rightarrow 1/8S_8 + H_2O + OCl^-$	$r_2 = k_2[H_2S][ClO_2^-]$	$k_2 = 0.4\ M^{-1}\ s^{-1}$ (fitted)
3	$1/4S_8 + 2ClO_2^- + OH^- \rightarrow S_2O_3^{2-} + OCl^- + HOCl$	$r_3 = k_3[ClO_2^-][OH^-]$	$k_3 = 4 \times 10^2\ M^{-1}\ s^{-1}$ (fitted)
4	$1/4S_8 + 2OCl^- + OH^- \rightarrow S_2O_3^{2-} + 2Cl^- + H^+$	$r_4 = k_4[OCl^-][OH^-]$	$k_4 = 1 \times 10^{11}\ M^{-1}\ s^{-1}$ (fitted)
5	$S_2O_3^{2-} + ClO_2^- + H_2O \rightarrow 2SO_3^{2-} + Cl^- + 2H^+$	$r_5 = k_5[S_2O_3^{2-}][ClO_2^-]$	$k_5 = 269\ M^{-1}\ s^{-1}$ (ref 20)
6	$HSO_3^- + ClO_2^- \rightarrow SO_4^{2-} + HOCl$	$r_6 = k_6[HSO_3^-][ClO_2^-]$	$k_6 = 27.2\ M^{-1}\ s^{-1}$ (ref 22)
7	$HSO_3^- + ClO_2^- + H^+ \rightarrow SO_4^{2-} + OCl^- + 2H^+$	$r_7 = k_7[HSO_3^-][ClO_2^-][H^+]$	$k_7 = 3.3 \times 10^8\ M^{-2}\ s^{-1}$ (ref 22)
8	$HOCl + 2ClO_2^- + H^+ \rightarrow 2ClO_2 + H_2O + Cl^-$	$r_8 = k_8[HOCl][ClO_2^-][H^+]$	$k_8 = 1.5 \times 10^6\ M^{-2}\ s^{-1}$ (ref 25)
9	$HOCl + ClO_2^- \rightarrow ClO_3^- + Cl^- + H^+$	$r_9 = k_9[HOCl][ClO_2^-]$	$k_9 = 1.2 \times 10^2\ M^{-1}\ s^{-1}$ (refs 25 and 26)
10	$S^{2-} + H_2O \rightarrow HS^- + OH^-$	$r_{10} = k_{10}[S^{2-}]$	$k_{10} = 100\ M^{-1}\ s^{-1}$ (ref 8)
11	$HS^- + OH^- \rightarrow S^{2-} + H_2O$	$r_{11} = k_{11}[HS^-][OH^-]$	$k_{11} = 100\ M^{-1}\ s^{-1}$ (ref 8)
12	$HS^- + H^+ \rightarrow H_2S$	$r_{12} = k_{12}[HS^-][H^+]$	$k_{12} = 7.5 \times 10^{10}\ M^{-1}\ s^{-1}$ (ref 8)
13	$H_2S \rightarrow HS^- + H^+$	$r_{13} = k_{13}[H_2S]$	$k_{13} = 4.3 \times 10^3\ s^{-1}$ (ref 8)
14	$HOCl \rightarrow H^+ + OCl^-$	$r_{14} = k_{14}[HOCl]$	$k_{14} = 3 \times 10^3\ s^{-1}$ (ref 22)
15	$H^+ + OCl^- \rightarrow HOCl$	$r_{15} = k_{15}[H^+][OCl^-]$	$k_{15} = 1.0 \times 10^{11}\ M^{-1}\ s^{-1}$ (ref 22)
16	$H_2O \rightarrow H^+ + OH^-$	$r_{16} = k_{16}[H_2O]$	$k_{16} = 1.0 \times 10^{-3}\ s^{-1}$ (ref [22])
17	$H^+ + OH^- \rightarrow H_2O$	$r_{17} = k_{17}[H^+][OH^-]$	$k_{17} = 1.0 \times 10^{11}\ M^{-1}\ s^{-1}$ (ref 22)
18	$HSO_3^- \rightarrow SO_3^{2-} + H^+$	$r_{18} = k_{18}[HSO_3^-]$	$k_{18} = 3.0 \times 10^3\ s^{-1}$ (ref 22)
19	$SO_3^{2-} + H^+ \rightarrow HSO_3^-$	$r_{19} = k_{19}[SO_3^{2-}][H^+]$	$k_{19} = 5.0 \times 10^{10}\ M^{-1}\ s^{-1}$ (ref 22)

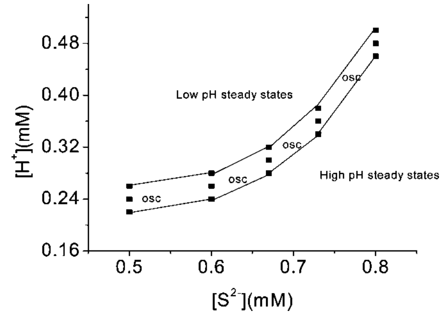

Figure 3. Phase diagram for the chlorite−sulfide−sulfuric acid system in the $[H_2SO_4]_0$−$[S^{2-}]_0$ parameter plane. $[NaClO_2]_0 = 1.0 \times 10^{-3}$ M, $k_0 = 0.73 \times 10^{-3}$ s^{-1}, and $T = 32$ °C.

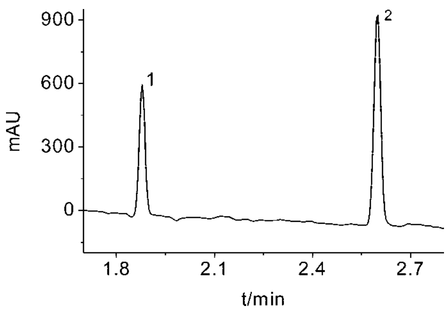

Figure 4. Electropherograms of the reaction solution at wavelength 214 nm, sampled at reaction time 40 min. Abscissa shows retention time on the CE column. Peaks represent (1) thiosulfate and (2) chlorite. Initial concentrations are 7.3×10^{-4} M Na_2S, 8.8×10^{-4} M $NaClO_2$, and 3.7×10^{-4} M H^+. The flow solvent was a buffer containing 1.6×10^{-2} M KH_2PO_4, 2.22×10^{-3} M $Na_2B_4O_7$, and 3.0×10^{-5} M CTAB.

2. Mechanistic Analysis. ***The Model.*** In order to describe the phenomena we observe in our experiments, we propose a model containing 19 reactions, which are summarized in Table 1. Our scheme involves two categories of reactions: 10 protonation (acid−base) equilibrium reactions and 9 redox reactions. With the exception of reactions 1−4, which we have fitted to our data, all rate constants are taken from the literature, as indicated in the table.

a. Essential Species. The following are the species that we found necessary to include in the mechanism.

HS^- and H_2S. The pK_a values for H_2S (pK_{a1} = 7.05, pK_{a2} = 19.00)[25] imply that the input sulfide exists almost completely as HS^- and H_2S, suggesting that $[S^{2-}]$ can be neglected. Both of these S(-II) species play important roles in the nonlinear mechanism.

S_8 and $S_2O_3^{2-}$. In the batch ClO_2^-−S^{2-} reaction at pH 6−8, a transient yellow color is seen, followed by a white turbid suspension that forms as the yellow disappears. The transient species is most likely polysulfide or polysulfur (S_8). Polysulfur has been observed in colloidal form in the S^{2-}−H_2O_2−H^+, S^{2-}−BrO_3^-−H^+, and S^{2-}−$S_2O_8^{2-}$−Ag^+ systems.[7,9,10] S_8 is treated in our model as a heterogeneous reactant that can be oxidized to $S_2O_3^{2-}$ through reactions 3 and 4 and then further oxidized to SO_3^{2-}. Thiosulfate is an important intermediate whose existence is confirmed by CE measurements (Figure 4).

SO_3^{2-} and HSO_3^-. These two species are important intermediates in the oxidation of sulfur compounds with low oxidation state to eventually yield SO_4^{2-}. As the pK_{a1} and pK_{a2} values of H_2SO_3 are reported to be 1.85 and 7.22, respectively,[25] formation of H_2SO_3 can be neglected, since the oscillation occurs at pH 4.5−5.5.

ClO_2^-, OCl^-, and HOCl. ClO_2^- is a major input species. OCl^- is produced by the reduction of ClO_2^-, which occurs at pH > 6. HOCl is formed by protonation of ClO^- in the oscillatory pH range. The formation of ClO_2 is accompanied by consumption of hydrogen ions, as shown in reaction 8.

H^+ and OH^-. These are key species in every pH-regulated oscillator. In our model, H^+ and OH^- come from two major sources: input reactants such as H_2SO_4 and as products of the various reactions.

b. Redox Reactions. Nine redox reactions are included in our model. These reactions and their corresponding rate constants at 32 °C are summarized in Table 1 (reactions 1−9). The rate constants for the first four of these have been obtained by fitting the simulations to our experiments; the remainder were taken from the literature.

Reactions 1 and 2 take place in neutral or weakly acidic media. Reactions 3 and 4 generate thiosulfate, which is then further oxidized to sulfite. As extremely rich nonlinear phenomena have been observed in the oxidation of thiosulfate by chlorite,[17−20] this reaction may play a key role in the nonlinear behavior exhibited by the present system. To verify the presence of thiosulfate, a solution identical to that in the CSTR was analyzed by CE at various times after the start of the reaction. As shown in Figure 4, besides the residual reactant ClO_2^- (peak 2), the major intermediate is thiosulfate (peak 1), as verified by comparison with a standard thiosulfate solution. We are unable to detect sulfite, sulfate, or sulfide, presumably because of their low UV absorbance. As shown in Figure 5, the thiosulfate peak area, that is, $[S_2O_3^{2-}]$, initially increases and then decreases after reaching a maximum at ~50 min, indicating that thiosulfate cannot be the final oxidation product.

Reaction 5 consumes $S_2O_3^{2-}$ and produces SO_3^{2-}. Nagypál et al.[19,20] investigated the reaction between $S_2O_3^{2-}$ and ClO_2^- and found a rate $r = k[S_2O_3^{2-}][ClO_2^-][H^+]$, $k = 1{-}2 \times 10^6$ M^{-2} s^{-1} at 25 °C and pH 6−9, which is equivalent to a value of k_5 = 1−2 M^{-1} s^{-1} at pH 6. Our experiments give k_5 = 10−100 M^{-1} s^{-1} at pH 5−6 and 32 °C. In our model, we set k_5 = 269.0 M^{-1} s^{-1}. Hydrogen ion is formed in reactions 4, 5, and 7. Reaction 7 is autocatalytic in H^+ and provides a positive feedback. Reactions 6 and 7 were studied by Frerichs et al.,[22] and we adopt their rate constants. Reaction 8 is a proton-consuming process, for which we use the rate law and rate constant reported by Peintler et al.[26] Reaction 9 is another H^+-formation process, which involves two steps:

$$HOCl + ClO_2^- + H^+ \rightarrow Cl_2O_2 + H_2O \tag{9a}$$

$$Cl_2O_2 + H_2O \xrightarrow{\text{fast}} ClO_3^- + Cl^- + 2H^+ \tag{9b}$$

$$r_{9a} = k_{9a}[HOCl][ClO_2^-][H^+] = k_9[HOCl][ClO_2^-],$$

$$k_9 = k_{9a}[H^+] \tag{9c}$$

The rate of reaction 9 is limited by reaction 9a, the rate-determining step. The value of k_{9a} is 1.1×10^6 M^{-2} s^{-1} at pH 5−6 and 25 °C,[26,27] which implies that $k_{9a}[H^+] = k_9$ is 1.1−11 M^{-1} s^{-1}. Under our experimental conditions, the pH oscillates between 5 and 6 at T = 32 °C, so $k_9 = k_{9a}[H^+]$ is expected to be larger than that at T = 25 °C. In our model, k_9 is taken to be 1.2×10^2 M^{-1} s^{-1}.

c. Protonation (Acid−Base) Equilibrium Reactions. Because the pK_a of HS^- exceeds 14, S^{2-} is never a major species in aqueous solution, since it hydrolyzes completely:

$$S^{2-} + H_2O \rightleftharpoons HS^- + OH^-$$

S^{2-} and its reaction with chlorite can thus be neglected. In acidic

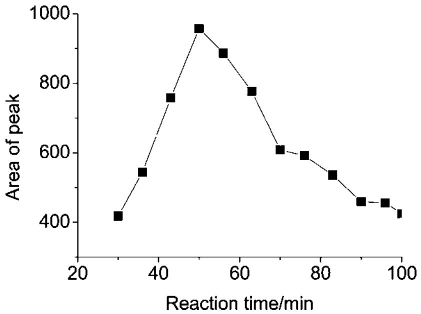

Figure 5. Variation of the thiosulfate peak area with time in the CE measurements. Initial concentrations are 7.0×10^{-4} M Na_2S, 1.8×10^{-4} M H_2SO_4, and 8.5×10^{-4} M $NaClO_2$.

medium, HS^- can combine with another proton to yield hydrogen sulfide:

$$HS^- + H^+ \rightleftharpoons H_2S$$

We take the rate constants for these reactions from a study of the hydrogen sulfide−hydrogen peroxide reaction.[8]

The protonation of sulfite is a critical process in our model. Protonated sulfite can be oxidized much faster than the unprotonated form. HSO_3^- cannot combine with another proton when pH > 4.0, since the pK_a of H_2SO_3 is 1.85.[27] As shown in Table 1, the rate constants of protonation reactions 10−13 are taken from ref 8, those of reactions 14−19 from ref 22.

3. Computer Simulations and Model Analysis. We simulated the behavior of the chlorite−sulfide reaction in sulfuric acid using the 19-step mechanism and corresponding parameters in Table 1. The simulation was carried out with a commercial software package (Berkeley Madonna,[28] error control parameter set at 1×10^{-10}) for stiff differential equations. As shown in Figure 1b, the period, amplitude, and waveform of the simulated oscillations agree well with the phenomena observed in the experiments. The simulations are also qualitatively consistent with the experiments in Figure 3, showing transitions from a low pH steady state to oscillations and then to a high pH steady state as the concentration of sulfide is increased. For example, with $[H^+]_0 = 0.30$ mM, the simulation gives the low pH state for $[S^{2-}]_0 < 0.7655$ mM, oscillations when 7.655 mM $< [S^{2-}]_0 < 0.7750$ mM, and the high pH state for $[S^{2-}]_0 > 0.7750$ mM.

Our simulations show that the rate of R8 is smaller than those of R2−R7 and R9 (see the Supporting Information) by several orders of magnitude. During the oscillations, the ratio of chlorite to chlorine dioxide always remains above 100 (see the Supporting Information). We also failed to observe chlorine dioxide in our batch experiments by UV−vis spectrophotometry. We have therefore neglected the oxidation of sulfur species by ClO_2 in our mechanism. In fact, both R1 and R8 can be deleted from the model without significantly modifying the oscillatory behavior. We include them, however, because they do have small effects on the amplitude and frequency of the simulated oscillations and because the species involved should be significant at pH 5−6.[25,26]

Conclusions

We have shown that sustained oscillations in pH and redox potential occur in the chlorite−sulfide system in a CSTR under appropriate conditions. In this new oscillator, an important negative feedback process is the oxidation of S(-II) to S(0) by ClO_2^-, and the key positive feedback process is the oxidation of S(IV) to S(VI) by ClO_2^-; that is, the oscillation is driven by the sulfur chemistry. The intermediate $S_2O_3^{2-}$, which has not previously been invoked in systems of this type, was detected here by CE measurements, and we propose reactions 3 and 4 to explain its formation. Based on our experiments, we suggest that the primary H^+-consumption processes involve the oxidation of sulfide (H_2S/HS^-) by ClO_2^- (reactions 1 and 2), in which elemental sulfur is produced, and the redox reaction between HOCl and ClO_2^- yielding ClO_2, Cl^-, and H_2O (reaction 6). In the processes where sulfur(IV) is oxidized to sulfur(VI) (reaction 7), hydrogen ions are released and autocatalysis occurs.

It is hoped that this research can lead toward new strategies for the treatment of sulfide-containing wastewater to decrease chemical oxygen demand and to reclaim valuable materials such as elemental sulfur.

Acknowledgment. This work was supported in part by the U.S. National Science Foundation (CHE-0615507), NSFC (Grant 20573134), NCET (Grant 05-0477) and JSNSF (BK2007037). Q.G. is grateful for the financial support of the visiting program of the Chinese Scholarship Council.

Supporting Information Available: Reaction rates for R1−R9; $[ClO_2^-]$ and $[ClO_2]$ as functions of time for a simulation of the reaction in a CSTR. This material is available free of charge via the Internet at http://pubs.acs.org.

References and Notes

(1) Buckley, A. N.; Hamilton, I. C.; Woods, R. *J. Electroanal. Chem.* **1987**, *216*, 213.
(2) Dorris, G. M. *Pulp Pap. Can.* **1969**, *95*, T394.
(3) Licht, S.; Manassen, J. *J. Electrochem. Soc.* **1987**, *134*, 1064.
(4) Lessner, P.; McLarnon, F. R.; Winnick, J.; Cairns, E. J. *J. Appl. Electrochem.* **1992**, *22*, 926.
(5) Ateya, B. G.; Al-Kharafi, F. M.; Abdallah, R. M.; Al-Azab, A. S. *J. Appl. Electrochem.* **2005**, *35*, 297.
(6) Burger, M.; Field, R. J. *Nature* **1984**, *307*, 720.
(7) Orbán, M.; Epstein, I. R. *J. Am. Chem. Soc.* **1985**, *107*, 2302.
(8) Rábai, G.; Orbán, M.; Epstein, I. R. *J. Phys. Chem.* **1992**, *96*, 5414.
(9) Simoyi, R. H.; Noyes, R. M. *J. Phys. Chem.* **1987**, *91*, 2689.
(10) Ouyang, Q.; De Kepper, P. *J. Phys. Chem.* **1987**, *91*, 6040.
(11) Rushing, C. W.; Thompson, R. C.; Gao, Q. *J. Phys. Chem. A* **2000**, *104*, 11561.
(12) Feng, J.; Gao, Q.; Xu, L.; Wang, J. *Electrochem. Commun.* **2005**, *7*, 1471.
(13) Alamgir, M.; Epstein, I. R. *Int. J. Chem. Kinet.* **1985**, *17*, 429.
(14) Scott, S. K.; Showalter, K. *J. Phys. Chem.* **1992**, *96*, 8702.
(15) Doona, C. J.; Blittersdorf, R.; Schneider, F. W. *J. Phys. Chem.* **1993**, *97*, 7258.
(16) Gao, Q.; Wang, J. *Chem. Phys. Lett.* **2004**, *391*, 349.
(17) Orbán, M.; De Kepper, P.; Epstein, I. R. *J. Phys. Chem.* **1982**, *86*, 431.
(18) Horváth, A. K.; Nagypál, I.; Epstein, I. R. *J. Am. Chem. Soc.* **2002**, *124*, 10956.
(19) Nagypál, I.; Epstein, I. R.; Kustin, K. *Int. J. Chem. Kinet.* **1986**, *18*, 345.
(20) Nagypál, I.; Epstein, I. R. *J. Phys. Chem.* **1986**, *90*, 6285.
(21) Alamgir, M.; Epstein, I. R. *J. Phys. Chem.* **1985**, *89*, 3611.
(22) Frerichs, G. A.; Mlnarik, T. M.; Grun, R. J. *J. Phys. Chem. A* **2001**, *105*, 829.
(23) Horváth, A. K.; Nagypál, I.; Peintler, G.; Epstein, I. R. *J. Am. Chem. Soc.* **2004**, *126*, 6246.
(24) Orbán, M. *React. Kinet. Catal. Lett.* **1990**, *42*, 343–353.
(25) Lide, D. R. *Handbook of Chemistry and Physics*, 83rd ed.; CRC Press: Boca Raton, FL, 2002; pp 8-44−8-45.
(26) Peintler, G.; Nagypál, I.; Epstein, I. R. *J. Phys. Chem.* **1990**, *94*, 2954.
(27) Horváth, A. K.; Nagypál, I.; Peintler, G.; Epstein, I. R.; Kustin, K. *J. Phys. Chem. A* **2003**, *107*, 6996.
(28) http://www.berkeleymadonna.com/.

JP807802V